Supplemental material to this article can be found at:
http://dmd.aspetjournals.org/content/suppl/2022/10/02/dmd.122.001041.DC1

1521-009X/50/12/1493–1500$35.00
DRUG METABOLISM AND DISPOSITION
U.S. Government Work not Protected by U.S. Copyright

dx.doi.org/10.1124/dmd.122.001041
Drug Metab Dispos 50:1493–1500, December 2022

Dimethandrolone, a Potential Male Contraceptive Pill, is Primarily Metabolized by the Highly Polymorphic UDP-Glucuronosyltransferase 2B17 Enzyme in Human Intestine and Liver[S]

Sheena Sharma, Deepak Ahire, Abdul Basit, Maria Lajoie, Christina Wang, Min S. Lee, Diana L. Blithe, John K. Amory, Dilip K. Singh, Scott Heyward, and Bhagwat Prasad

Department of Pharmaceutical Sciences, Washington State University, Spokane, Washington (S.S., D.A., A.B., D.K.S., B.P.); The Lundquist Institute at Harbor UCLA Medical Center, Torrance, California (M.L., C.W.); Contraceptive Development Program, Eunice Kennedy Shriver National Institute of Child Health and Human Development, National Institutes of Health, Bethesda, Maryland (M.S.L., D.L.B.); Department of Medicine, University of Washington School of Medicine, Seattle, Washington (J.K.A.); and BioIVT, Halethorpe, Maryland (S.H.)

Received July 21, 2022; accepted September 6, 2022

ABSTRACT

Dimethandrolone undecanoate (DMAU), an oral investigational male hormonal contraceptive, is a prodrug that is rapidly converted to its active metabolite, dimethandrolone (DMA). Poor and variable oral bioavailability of DMA after DMAU dosing is a critical challenge to develop it as an oral drug. The objective of our study was to elucidate the mechanisms of variable pharmacokinetics of DMA. We first identified DMA metabolites formed in vitro and in vivo in human hepatocyte incubation and serum samples following oral DMAU administration in men, respectively. The metabolite identification study revealed two metabolites, DMA-glucuronide (DMA-G; major) and the androstenedione analog of DMA (minor), in the hepatocyte incubations. After oral DMAU administration, only DMA-G was detected in serum, which was >100-fold compared with DMA levels, supporting glucuronidation as the major elimination mechanism for DMA. Next, 13 clinically relevant UDP-glucuronosyltransferase (UGT) enzymes were tested for their involvement in DMA-G formation, which revealed a major role of UDP-glucuronosyltransferase 2B17 (UGT2B17) isoform with a smaller contribution of UGT1A9 in DMA-G formation. These data were confirmed by dramatically higher DMA glucuronidation rates (>200- and sevenfold) in the high versus the null UGT2B17-expressing human intestinal and liver microsomes, respectively. Since human UGT2B17 is a highly variable enzyme with a 20%–80% gene deletion frequency, the in vitro data suggest a major role of UGT2B17 polymorphism on the first-pass metabolism of DMA. Further, considering DMA is a selective and sensitive UGT2B17 substrate, it could be used as a clinical probe of UGT2B17 activity.

SIGNIFICANCE STATEMENT

Dimethandrolone (DMA) is an active metabolite of dimethandrolone undecanoate (DMAU), an investigational male hormonal contraceptive. Previous studies have indicated poor and inconsistent bioavailability of DMAU following oral administration. This study found that UDP-glucuronosyltransferase 2B17–mediated high intestinal first-pass metabolism is the key mechanism of variable DMA bioavailability.

Introduction

In the United States, only 30% of couples use a male method of contraception, with 20% using condoms for contraception and 10% relying on vasectomy (Daniels et al., 2015). This necessitates the need for developing a safe and reversible male contraceptive to reduce the disparity in contraception use and to encourage equal participation of both the sexes in family planning (Amory, 2020). Ideally, an oral male pill could offer the most convenient and accessible contraceptive option to men. Unfortunately, attempts to use oral testosterone as contraceptive failed because it is cleared too rapidly as a single daily dose regimen even in combination with progestin analogs, whereas multiple doses of oral testosterone per day would be impractical for contraception (Blithe, 2016). Although 17-methyltestosterone has good oral bioavailability, its long-term use has been associated with hepatotoxicity (Westaby et al., 1977).

This work was supported by *Eunice Kennedy Shriver* National Institute of Child Health and Human Development via a subcontract through The Lundquist Institute (Contract: HHSN27520130024I; Task Order: HHSN27500004; C.W.).

The authors declare no conflict of interest.

dx.doi.org/10.1124/dmd.122.001041.

[S] This article has supplemental material available at dmd.aspetjournals.org.

ABBREVIATIONS: AUC, area under the systemic concentration-time profile curve; BSA, bovine serum albumin; CE, collision energy; CNV, copy number variation; DDI, drug-drug interaction; DMA, dimethandrolone; DMA-G, DMA-glucuronide; DMAU, dimethandrolone undecanoate; $f_{m,UGT2B17}$, drugfraction glucuronidated by UGT2B17; HI, hepatocyte incubation; HIM, human intestinal microsome; HLM, human liver microsome; HT, hepatocyte thawing; LC-HRMS, liquid chromatography–high-resolution mass spectrometry; LC, liquid chromatography; LC-MS, Liquid chromatography-mass spectrometry; LC-MS/MS, liquid chromatography with tandem mass spectrometry; MeCN, acetonitrile; MRM, multiple reaction monitoring; PK, pharmacokinetic; QC, quality control; rhUGT, recombinant human UGT; rhUGT2B17, recombinant human UGT2B17; T/E, testosterone-to-epitestosterone ratio; TG, testosterone glucuronide; UDPGA, UDP–glucuronic acid; UGT2B17, UDP-glucuronosyltransferase 2B17.

Thus, an oral male contraceptive with a longer duration of action is an unmet need.

Dimethandrolone undecanoate (DMAU; 7α,11β-Dimethyl-19-nortestosterone 17β-undecanoate) is a promising experimental male hormonal contraceptive. DMAU is a prodrug that is metabolized to its active metabolite, dimethandrolone (DMA) (Surampudi et al., 2014; Ayoub et al., 2017; Thirumalai et al., 2019) (Fig. 1A). DMA binds to both the androgen and the progesterone receptors and hence can be potentially used as a single-agent male contraceptive (Attardi et al., 2011) (Fig. 1B). However, the poor and variable oral bioavailability of DMAU (and DMA), including the first-pass metabolism and positive food effect [13- and sixfold area under the systemic concentration-time profile curve (AUC) of DMAU and DMA in fed compared with fasting states] (Surampudi et al., 2014; Ayoub et al., 2017), is a critical challenge affecting its potential success as an oral drug. Moreover, DMAU and DMA are highly lipophilic (logP 6.5 and 3.9, respectively) and poorly water soluble (4.4×10^{-5} and 0.0293 mg/ml, respectively) (Attardi et al., 2011; Ayoub et al., 2017). Poor solubility could be a possible reason for the poor DMA bioavailability; however, the role of first-pass metabolism of DMA has not been ruled out. In particular, DMA and testosterone are structurally similar (Fig. 1C), and importantly, DMA retains the 17β-hydroxy group, and therefore, it is highly susceptible to glucuronidation in the intestine and liver. Testosterone is extensively metabolized in human enterocytes and hepatocytes to multiple primary metabolites, including androstenedione, testosterone glucuronide (TG), and 6-hydroxy testosterone, by hydroxysteroid 17-β dehydrogenase 2, UDP-glucuronosyltransferase 2B17 (UGT2B17), and cytochrome P450 3A4, respectively(Zhang et al., 2018). Among these metabolites, TG is one of the predominant metabolites after oral administration, with >80-fold exposure in men compared with testosterone levels, and UGT2B17 is the main enzyme involved in testosterone-to-TG conversion (Basit et al., 2018). UGT2B17 is predominantly more expressed in the human intestine than in the liver, and copy number variation (CNV) in its gene has been shown to be associated with interindividual variability in the urinary excretion of TG (Jakobsson et al., 2006; Schulze et al., 2008) and drug metabolism, including first-pass metabolism (Wang et al., 2012; Basit et al., 2018). Therefore, we hypothesized that extensive first-pass metabolism of DMA is the primary mechanism of its poor and variable bioavailability, and UGT2B17 is the major enzyme that converts DMA to DMA-glucuronide (DMA-G). We investigated the in vitro and in vivo metabolic profiling of DMA to elucidate the mechanisms leading to its variable pharmacokinetics (PK). First, we identified DMA metabolites formed in human hepatocyte incubation and in serum samples after oral DMAU dosing by liquid chromatography–high-resolution mass spectrometry (LC-HRMS). Second, we elucidated UGT isoforms involved in DMA glucuronidation. Finally, we determined the effect of UGT2B17 gene deletion on DMA metabolism in human intestinal and liver microsomes (HIM and HLM, respectively) and quantified the fraction of DMA metabolized by a specific enzyme (f_m) in the intestine and liver. The in vitro findings were confirmed through in vivo PK analysis of human serum samples from an oral PK study of DMAU. Overall, this mechanistic study explains challenges with the oral bioavailability of DMA and provides insights into developing better approaches for DMAU oral delivery.

Materials and Methods

Chemicals, Reagents, and Software

DMAU, DMA, and their respective stable-labeled (d5-deuterated) standards were obtained through Dr. Min Lee (*Eunice Kennedy Shriver* National Institute of Child Health and Human Development) from Ash Stevens (Riverview, MI). Liquid chromatography-mass spectrometry (LC-MS)–grade acetonitrile (MeCN), methanol, chloroform, and formic acid were purchased from Fisher Scientific (Fair Lawn, NJ). Alamethicin, UDP–glucuronic acid (UDPGA), magnesium chloride, and dibasic and monobasic potassium phosphate were purchased from Sigma-Aldrich (St. Louis, MO). Ammonium bicarbonate (98% pure), bovine serum albumin (BSA), dithiothreitol, iodoacetamide, and trypsin were procured from Thermo Fisher Scientific (Rockford, IL). Oasis HLB cartridges were purchased from Waters (Milford, MA). Testosterone, TG, and their respective stable-labeled (d3-deuterated) standards were purchased from Cerilliant Corporation (Round Rock, TX). Male human plateable cryopreserved hepatocytes (Product number M00995; $n = 3$) were obtained from BioIVT (Westbury, NY), and hepatocyte thawing (HT) and hepatocyte incubation

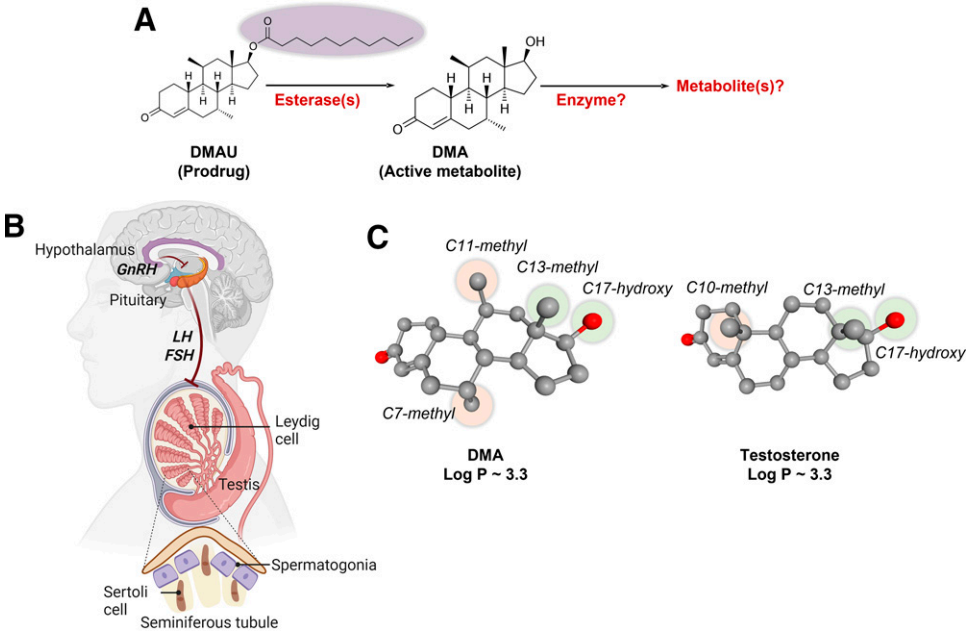

Fig. 1. (A) DMAU is an ester prodrug that is rapidly metabolized to its active metabolite, DMA. Sequential metabolism of DMA is not well characterized. (B) The mechanism of action of DMAU involves suppression of follicle-stimulating hormone (FSH) and luteinizing hormone (LH) secretion from the pituitary gland, leading to a cessation of spermatogenesis. (C) Chemical structures of DMA and testosterone.

(HI) media were procured from Invitrogen (Waltham, MA). Recombinant human UGT (rhUGT) enzymes were procured from Corning Life Sciences (Corning, NY). Pooled HIM and HLM (mix of male and female subjects) were obtained from Xenotech (Kansas City, KS). Individual genotyped and deidentified (i.e., identifiable donor information such as donor name was unknown to us) HLM samples were from our previous study (Zhang et al., 2018) and were procured from the University of Washington School of Pharmacy Liver Bank (Seattle, WA). Synthetic light (with amino acid analysis) and stable isotope-labeled peptides were purchased from New England Peptides (Boston, MA) and Thermo Fisher Scientific, respectively. MATLAB (Natick, MA), BioRender (Toronto, Ontario), GraphPad (San Diego, CA), XCMS Online (Scripps Research; San Diego, CA), and Microsoft Office Excel and PowerPoint (Redmond, WA) were used to create the figures or data analysis.

DMA Metabolism in Human Hepatocytes

Cryopreserved human hepatocytes were thawed and plated according to a previously defined protocol (Basit et al., 2018). Briefly, the HT and HI media were warmed at 37°C for 30 minutes. The hepatocyte vial was completely thawed by immersing it into a 37°C water bath. Thawed hepatocytes were poured gently into the HT medium in a 50 ml conical tube, mixed by gently inverting few times, and centrifuged at 100*g* for 10 minutes at room temperature. The cell pellet was gently resuspended in 3 ml of HT medium, and hepatocytes were counted using the Trypan Blue exclusion method using Auto T4 cellometer (Nexcelom Bioscience, Lawrence, MA). HI medium was added to the cell suspension to make 1×10^6 cells per ml concentration. The reactions were initiated by adding 500 µl of hepatocyte suspension to 500 µl of prewarmed HI medium containing 5 µl of 15, 2, and 0.2 µM DMA, separately, in 6-well plates ($n = 3$ individual hepatocytes) (Supplemental Table 1), i.e., final cell count of 0.5×10^6 cells per well and a final concentration of 0.1, 10, and 75 µM DMA. The 6-well plates were kept into a 37°C incubator maintained at 5% CO_2 immediately after seeding. The reaction was quenched with a fivefold higher volume of ice-cold MeCN containing internal standard (heavy isotope–labeled DMA-d5) compared with the total sample volume at 60 and 120 minutes. The sample was vortexed for 1 minute to extract all the metabolites, followed by centrifugation at 3000*g* for 10 minutes (4°C). The supernatant was subjected to freezing (−20°C) until both MeCN and aqueous layers became immiscible and the aqueous layer was frozen. The upper MeCN layer (drug and nonpolar metabolites) was collected in another tube. The lower aqueous layer (polar metabolites) was subjected to solid-phase extraction using HLB cartridge. The procedure involved cartridge conditioning with 2 ml methanol followed by 2 ml water containing 0.2% formic acid, loading of samples (0.5 ml), washing with 1 ml water containing 2% methanol and 0.2% formic acid, and elution of the analytes with 0.5 ml MeCN. Finally, aliquot from solid-phase extraction was pooled with the previously collected MeCN layer. The mixtures were dried at 40°C using a nitrogen evaporator (Techne, Minneapolis, MN), and the dried samples were reconstituted in 100 µl of 70:30 MeCN:water (0.1% formic acid) and centrifuged at 10,000*g* for 10 minutes. The supernatant was stored at −80°C prior to liquid chromatography with tandem mass spectrometry (LC-MS/MS) analysis.

DMA Metabolism in Human Serum

The representative serum samples ($n = 3$ males) (Supplemental Table 2) were available to us from a previous clinical study (Ayoub et al., 2017) conducted at the Lundquist Institute at Harbor-UCLA Medical Center. The clinical study was approved by the institutional review board, and the study details are reported previously (Surampudi et al., 2014; Ayoub et al., 2017). The subjects were given a 100 mg dose of oral DMAU in castor oil with a high fat meal (>50% fat, 800–900 calories, with approximately 150, 250, and 500–600 calories of protein, carbohydrates, and fat, respectively). For the metabolite characterization, a pooled sample (20 µl) at each time point, specifically 0.5, 1, 2, 4, 6, 8, 12, and 18 hours after oral administration, was mixed with 90 µl of ice-cold MeCN containing 0.1% formic acid and 25 ng/ml of internal standard (DMA-d5). The sample was vortex mixed and centrifuged at 10,000*g* for 10 minutes (4°C). Ten µl of the supernatant was collected and added with 50 µl of water containing 0.1% formic acid and transferred to a liquid chromatography (LC) vial for LC-HRMS analysis.

DMA Metabolite Identification in Human Hepatocyte and Serum Samples

Prior to the analysis of DMA metabolites, a list of structurally feasible metabolites was generated using the testosterone metabolic profile as described previously (Basit et al., 2018; Zhang et al., 2018) (Table 1). A targeted data-dependent metabolomics approach was used to screen the predicted metabolites of DMA. Other than predicted metabolite structures of DMA, untargeted metabolomics was performed by comparing high-resolution MS data of pre- and postdose samples using XCMS Online. The following screening criteria were employed to filter potential metabolites: 1) a postdose sample with >10-fold response compared with the predose sample, 2) a mass defect filter (miili dalton range from −50 to 50, 3) a retention time window of 20–46 minutes (considering highly polar DMA-G was observed at about 27 minutes), and 4) an MS intensity of $>10^6$ in postdose sample and MS intensity of $<10^6$ in predose sample.

Both in vitro (hepatocyte incubation) and in vivo (serum) samples were analyzed using Thermo Scientific Q Exactive HF Nanoflow LC in data-dependent acquisition mode. Chromatographic separation of metabolites was achieved using a Thermo Reversed Phase Nano C18 Column (75 × 250 mm, 2 µm particle size). LC conditions were set at a 300 nl/min flow rate and 1 µl injection volume with mobile phase A: water with 0.1% formic acid and B: MeCN with 0.1% formic acid. The gradient was as follows: 0.0–5.0 minutes (5% B), 5.0–20.0 minutes (5%–50% B), 20.0–35.0 minutes (50%–80% B), 35.0–45.0 minutes (80%–80% B), 45.0–46.0 minutes (80%–90% B), 46.0–56.0 minutes (90%–90% B), and 56.0–57.0 minutes (90%–5% B), followed by an 8-minute gradient of 5% B. The mass spectrometer was operated in full MS and data-dependent MS^2 in the positive polarity mode with a scan range of 250–1000 m/z and 200–2000 m/z for full MS and MS^2, respectively (Supplemental Table 3).

In Vitro Characterization of DMA Glucuronidation Enzyme

UGT Screening Assay of DMA. Thirteen UGT enzymes were tested for their potential to form DMA-G. These enzymes include UGT1A1, 1A3, 1A4, 1A6, 1A7, 1A8, 1A9, 1A10, 2B4, 2B7, 2B10, 2B15, and 2B17. Briefly, an 80 µl mixture of alamethicin (2 mg/ml), BSA (0.2%, 2 mg/ml), and 5 mM $MgCl_2$ /100 mM potassium phosphate buffer (pH 7.4) (1:1:14, respectively) was added, followed by the addition of 5 µl of 0.2 mg/ml rhUGT enzymes to a 96-well plate. Next, 10 µl of DMA (100 µM) was added and kept on ice for 15 minutes, followed by initialization of the reaction by adding 5 µl of 50 mM UDPGA and incubation for 45 minutes (37°C) at 300 rpm. The reaction was quenched using 200 µl ice-cold MeCN containing TG-d3 as internal standard. The samples were centrifuged at 2000*g* for 5 minutes (4°C), and the supernatant was transferred to an LC vial. The reaction was performed in triplicates.

DMA-G Assay in Recombinant Human UGT2B17, HIM, and HLM. DMA-G assay was performed in recombinant human UGT2B17 (rhUGT2B17), HIM, and HLM. For DMA-G kinetic assays, a similar experimental procedure

TABLE 1

Predicted DMA metabolites assessed in human hepatocyte and serum samples after the oral administration of DMAU and their exact masses

Metabolites	Exact Mass [M+H]
17-DMA estradiol	271.1693
17-DMA estradiol-3-glucuronide	463.1963
17-DMA estradiol-glucuronide	463.1963
5α-Dihydro DMA	305.2475
6-OH-DMA	319.2268
Dihydro DMA-glucuronide	481.2796
DMA 3-sulfate	383.1887
DMA androstenedione	303.2319
DMA androstenedione	301.2162
DMA androsterone	305.2475
DMA androsterone-glucuronide	481.2796
DMA epiandrosterone	305.2475
DMA epiandrosterone-glucuronide	481.2796
DMA estrone	269.1536
DMA estrone-glucuronide	463.1963
DMA etiocholanediol	307.2632
DMA etiocholanolone	305.2475
DMA etiocholanolone-glucuronide	481.2796
DMA-cysteine conjugate	422.2359
DMA-glucuronide	479.2639
DMA-glutathione conjugate	608.3000

was followed as discussed above with DMA concentration ranging from 0.2 to 100 μM. After 15 minutes of pretreatment on ice, reactions were initiated by the addition of 5 μl of 50 mM UDPGA, incubated for 30 minutes (37°C) at 300 rpm, and the reaction was terminated using 200 μl of ice-cold MeCN containing TG-d3. The samples were then centrifuged at 2000*g* for 5 minutes (4°C), and the supernatant was collected in an LC vial for the analysis. The reaction was performed in triplicates.

Preparation of Stock Solutions, Calibration Standards, and Quality Controls for Analysis. A mix of stock solutions of DMA and DMAU (1:10) was serially diluted into 13 working standards in methanol (0.06–250 ng/ml and 0.61–2500 ng/ml, respectively). Ten μl working standard solution was spiked into 40 μl of blank biologic matrix (human plasma:water, 50:50 v/v), and protein was precipitated by adding 200 μl of the internal standard (25 ng/ml DMA-d5 in methanol). The sample was vortex mixed for 15 seconds, followed by centrifugation at 15,000*g* (4°C), and the supernatant was collected for MS and Data Analysis of in Vitro DMA Kinetics Samples analysis. Similarly, quality-control (QC) samples representing three concentrations were prepared (low: 0.12 and 0.01 pg/ml; medium: 7.8 and 0.78 pg/ml; and high: 500 and 50 pg/ml, DMAU and DMA, respectively).

Because DMA-G standard was not available, we used a surrogate standard method to analyze DMA-G in in vitro hepatocyte incubations and serum samples. Here, testosterone and TG calibration standards (2, 10, 25, and 50 ng/ml) were prepared in methanol, and the ratio of TG/testosterone response was used as a surrogate of DMA-G/DMA response using identical MS parameters.

LC-MS/MS and Data Analysis of in Vitro DMA Kinetics Samples. Samples were centrifuged at 10,000*g* for 5 minutes (4°C), and the supernatant (150 μl) was collected and transferred to an LC vial for analysis by MS instrument connected to a standard/MS (Waters Xevo-TQ-XS MS; Waters, Milford, MA) with standard electrospray ionization source, microflow LC, and Acquity UPLC HSS T3 column (100Å, 1.8 μM, 1 mm × 100 mm). LC conditions were set at a 40 μl/min flow rate and 1 μl injection volume using mobile phase A: water with 0.1% formic acid and B: MeCN with 0.1% formic acid, using the following gradient program: 0.0–0.5 minutes (30% B), 0.5–3.5 minutes (30%–98% B), 3.5–7.0 minutes (98%–98% B), and 7.0–7.1 minutes (98%–30% B), followed by a 1.9-minute gradient of 30% B. The mass spectrometer was operated in multiple reaction monitoring (MRM) and positive ion mode with a cone voltage of 30 V. The MRM transitions were: DMA-G [m/z 479.3→ 285.4 and 303.2; collision energy (CE) 25 eV], TG-d3 (m/z 468.2→ 97.1 and 109.1; CE 40 eV), testosterone (m/z 289.2→ 97 and 109; CE 40 eV), and TG (m/z 465.3→ 271.2 and 289.2; CE 25 eV).

Enzyme kinetic parameters (K_m and V_{max}) were obtained by fitting the Michaelis-Menten equation using GraphPad Prism v. 8.4.3 (eq. 1), where Y is DMA-G formation rate, and X is DMA concentration.

$$Y = \frac{V_{max} * X}{(K_m + X)} \quad (1)$$

MS instrument connected to a standard/MS Protein Quantification of UGT1A9 and UGT2B17 Proteins in HIM and HLM. We applied an optimized targeted LC-MS/MS methodology to selectively quantify UGT1A9 and UGT2B17 enzymes (Ahire et al., 2021). Peptide selection for the proteins was performed using a previously discussed in silico approach (Prasad et al., 2019). Total protein concentration was quantified using a BCA assay kit (Pierce Biotechnology, Rockford, IL) following the vendor protocol, and the proteins were digested as described previously (Ahire et al., 2021). Briefly, 80 μl of the tissue sample (1 mg/ml total protein) was mixed with 30 μl ammonium bicarbonate (100 mM) and 20 μl of BSA (0.02 mg/ml) in a 1.5 ml microcentrifuge tube. Proteins were denatured and reduced with 10 μl of 250 mM dithiothreitol at 95°C for 10 minutes with gentle shaking at 300 rpm. The sample was cooled at room temperature for 10 minutes, and the denatured protein was alkylated with 10 μl of 100-mM iodoacetamide in the dark for 30 minutes. One ml of ice-cold acetone was added to each sample, followed by vortex mixing and incubation at −80°C for 30 minutes. Next, the sample was centrifuged at 16,000*g* (4°C) for 10 minutes and the supernatant was carefully removed using vacuum suction. The protein pellet was dried at room temperature for 30 minutes and washed with 500 μl ice-cold methanol, followed by centrifugation at 16,000*g* (4°C) for 10 minutes. The supernatant was removed and the pellet was dried at room temperature for 30 minutes and resuspended in 60 μl ammonium bicarbonate buffer (50 mM, pH 7.8). Finally, the reconstituted protein sample was digested by adding 20 μl of trypsin (protein:trypsin ratio, approximately 50:1) and incubated for 16 hours at 37°C. The sample was centrifuged at 1000*g* (4°C) for 1 minute and kept in −20°C for 5 minutes. Then, the reaction was quenched by the addition of 10 μl of peptide internal standard cocktail (prepared in 80% MeCN in water containing 0.5% formic acid) and 5 μl of 5% formic acid in water. The sample was vortex mixed and centrifuged at 4000*g* for 5 minutes. The supernatant was collected in an LC-MS vial for analysis. LC-MS/MS data acquisition was performed on an M-class Waters UPLC system coupled with a Waters Xevo TQ-XS microflow LC-MS/MS instrument connected to a standard electrospray ionization source using optimized parameters outlined in Supplemental Tables 4 and 5. The peptides were separated on a standard HSS T3 C18 column (1.8 μm, 1.0 × 100 mm). All samples were digested and analyzed in triplicate. The proteotypic peptides of UGT1A9 (AFAHAQWK) and UGT2B17 (FSVGYTVEK and SVINDPIYK) were quantified in the digested samples using a validated LC-MS/MS method (Ladumor et al., 2019; Ahire et al., 2021). Light peptides were used as calibrators, and the corresponding heavy peptides containing terminal-labeled [$^{13}C_6$ $^{15}N_2$]-lysine or [$^{13}C_6$ $^{15}N_4$]-arginine residues served as internal standards.

Calculation of the Fractional Metabolism of DMA. The f_m values were calculated using the V_{max} values from high- and null-expressing HIM and HLM experiments (eqs. 2 and 3), where $f_{m,UGT2B17}$ and $f_{m,non\text{-}UGT2B17}$ are the fractions of DMA glucuronidated by UGT2B17, and non-UGT2B17 enzymes, respectively.

$$f_{m,\,UGT2B17} = \frac{V_{max,\,high\ UGT2B17\ expressing\ HIM\ or\ HLM} - V_{max,\,null\ UGT2B17\ expressing\ HIM\ or\ HLM}}{V_{max,\ high\ UGT2B17\ expressing\ HIM\ or\ HLM}} \quad (2)$$

$$f_{m,\,non-UGT2B17} = \frac{V_{max,\,null\ UGT2B17\ expressing\ HIM\ or\ HLM}}{V_{max,\,high\ UGT2B17\ expressing\ HIM\ or\ HLM}} \quad (3)$$

Analysis of DMA in Human Serum Samples and PK Analysis

Sample Preparation and LC-MS/MS Analysis. We adopted a previously reported method (Surampudi et al., 2014; Ayoub et al., 2017) for DMA quantification in human serum samples, with a few modifications. Briefly, for the

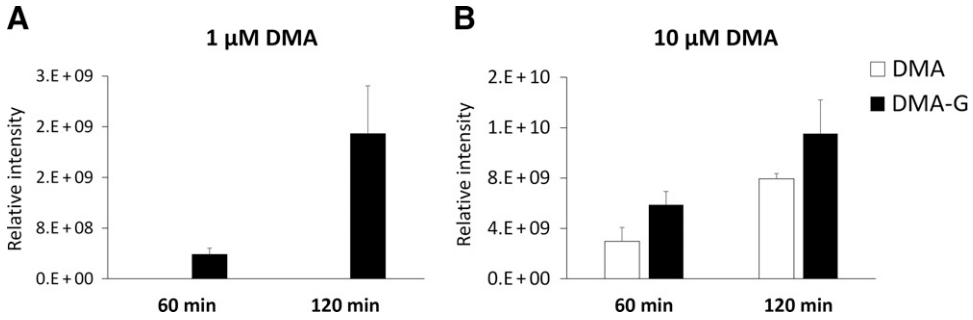

Fig. 2. The relative amounts of DMA (open bar) and DMA-G (filled bar) formed in human hepatocytes at (A) 1 μM and (B) 10 μM DMA concentrations at 60 and 120 minutes. No DMA was detected at 1 μM DMA incubation, suggesting its rapid elimination to form DMA-G. The ratios of DMA-G to DMA concentrations were twofold at 10 μM hepatocyte incubations, confirming higher formation of the metabolite compared with the parent.

analysis of PK samples from three individuals, 25 µl of serum sample was diluted twofold with water, and the internal standard (200 µl of 25 ng/ml DMA-d5) was added. The sample was vortex mixed for 15 seconds, followed by centrifugation at 15,000*g* for 10 minutes (4°C). The supernatant (150 µl) was collected and transferred to an LC vial for analysis by LC-MS/MS (M-class LC coupled to Waters Xevo-TQ-XS).

The LC-MS conditions used for analyzing human serum samples were similar to those shown for the in vitro DMA kinetics sample analysis above, except that the injection volume was 2 µl. For additional analytes, the MRM transitions were DMA (m/z 303.2→ 97 and 109; CE 40 eV) and DMA-d5 (m/z 308.3→ 102 and 114; cone voltage 30; CE 40 eV).

The method for DMA quantification was validated for linearity, dynamic range accuracy, and analytical range. The method was linear (r^2 = 0.9956), with the accuracy of 97%, 112%, and 106%, corresponding to DMA concentrations of 0.8 ng/ml (low concentration QC), 6.25 ng/ml (medium concentration QC), and 12.5 ng/ml (high concentration QC), respectively. The lower limit of

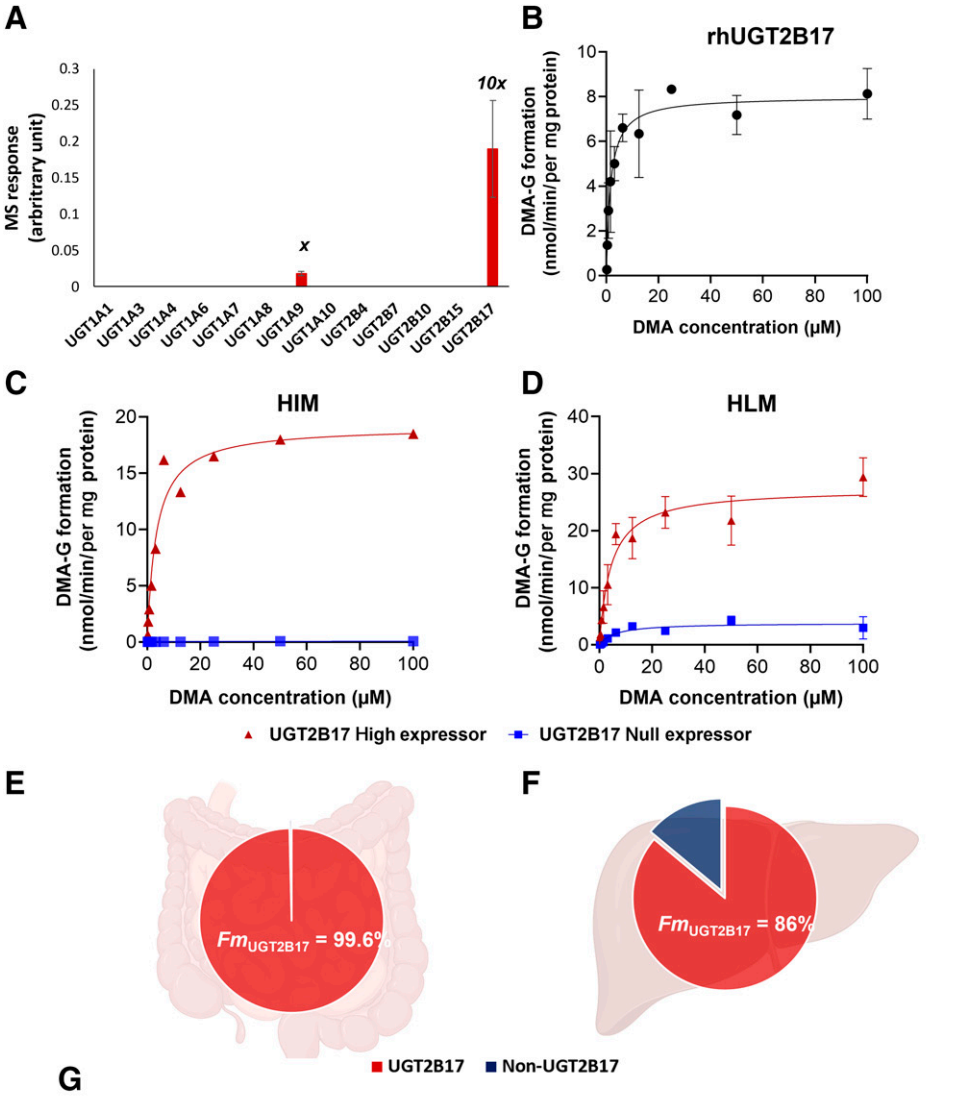

G

Parameter (95% CI)	rhUGT2B17	HIM – High UGT2B17 expressing	HIM – Null UGT2B17 expressing	HLM – High UGT2B17 expressing	HLM – Null UGT2B17 expressing
V_{max} (nmol/min/per mg protein)	8 (7.3–8.7)	19.1 (16.8–21.8)	0.07 (0.04–0.12)	27.4 (23.9–31.4)	3.8 (2.9–4.9
K_m (µM)	1.63 (1.1–2.5)	3.4 (2.1–5.7)	12.7 (2.3–61.1)	4.4 (2.5–7.4)	5.9 (2.4–14.6)
UGT2B17 abundance (pmol/mg protein)	39.65	21.63	0	8.5	0

Fig. 3. (A) MS response of DMA-G formation in 13 rhUGT2B17 enzymes. UGT1A9 and UGT2B17 were the only enzymes involved in DMA metabolism. (B) DMA metabolism kinetics in the rhUGT2B17 system. (C and D) DMA-G formation kinetics in the high (red) versus null (blue) UGT2B17-expressing HIM (n = 2 high expressors and n = 3 low expressors) and HLM (n = 3 high and null expressors). The data points represent the mean ± standard deviation. (E and F) The estimated $f_{m,\ UGT2B17}$ was 99.6% and 86%, respectively, in the high-expressing intestinal and liver microsomes, respectively. (G) Michaelis-Menten parameters and UGT2B17 protein abundance in rhUGT2B17 and the high versus null UGT2B17-expressing HIMs and HLMs, respectively.

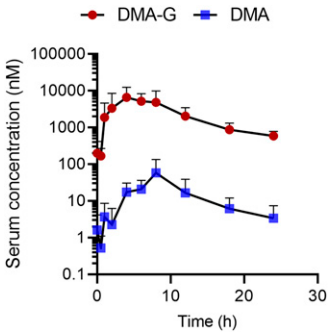

Fig. 4. Pharmacokinetic profiles of DMA-G (red circle) and DMA (blue square) following an oral administration of 100 mg DMAU. The systemic exposure (AUC) of DMA-G was >100-fold than DMA serum concentrations, confirming glucuronidation as the major mechanism of DMA disposition.

quantification was 0.4 ng/ml, and the upper limit of quantification was 50 ng/ml. The response of the stable isotope-labeled internal standard (DMA-d5) was consistent across samples. Because the synthetic standard of DMA-G was not available, a surrogate standard approach was used for DMA-G quantification (eq. 4). The ratio of TG to testosterone was used for DMA-G quantification, assuming that the glucuronidation results in similar changes in the mass ionization efficiencies of DMA, and for testosterone, assuming that the critical LC-MS/MS parameters remains similar between the pairs (aforementioned).

$$[\text{DMA} - \text{G concentration}] = [\text{DMA concentration}] \times \frac{\text{TG MS response}}{\text{Testosterone MS response}} \quad (4)$$

Pharmacokinetic Data Analysis. The calculation of PK parameters was performed via MATLAB R2021b software through noncompartmental PK analysis. All data were expressed as mean ± S.D.

Results

Metabolite Characterization of DMA in Human Hepatocyte and Serum Samples. We first leveraged the testosterone metabolic profile to predict the plausible structures of DMA metabolites. Out of 21 structurally feasible metabolites of DMA, only DMA-G (m/z 479.2639) and androstenedione analog of DMA (m/z 301.2162) were formed in hepatocyte incubations, but only DMA-G was detected in human serum samples following an oral dose of 100 mg DMAU (Table 1; Supplemental Fig. 1). In addition, differences in metabolomics profiles of pre- and postdose serum samples were evaluated using XCMS software, which further confirmed DMA-G as the predominant metabolite. Although untargeted metabolomics data showed some additional species (Supplemental Table 6), they were either found in both pre- and postdose samples, small in abundance, or were potentially endogenous metabolites likely affected by the treatment. Interestingly, other predicted metabolites based on testosterone metabolite profile were not detected (or were below the limit of quantification) following DMA or DMAU incubations. The LC-HRMS analysis of human hepatocyte and serum samples confirmed that glucuronidation is the major biotransformation pathway involved in DMA metabolism (Supplemental Fig. 1). No DMA was detected at 1 μM DMA incubation, suggesting its rapid elimination to DMA-G. The ratio of DMA-G to DMA concentrations was ∼twofold at 10 μM hepatocyte incubations, confirming higher formation of the metabolite compared with the parent (Fig. 2). In addition, both DMA-G and androstenedione analogs to parent ratios were comparable in both DMA and DMAU incubations, indicating that DMAU to DMA formation is not the rate-limiting step (Supplemental Fig. 2).

UGT Screening Assay of DMA. Out of the 13 clinically relevant rhUGT enzymes (UGT1A1, 1A3, 1A4, 1A6, 1A7, 1A8, 1A9, 1A10, 2B4, 2B7, 2B10, UGT2B15, and 2B17) that were tested for their capacity to metabolize DMA, only UGT2B17 and UGT1A9 were found to metabolize DMA to DMA-G. DMA-glucuronidation rate was 10-fold in rhUGT2B17 as compared with in rhUGT1A9 incubations (Fig. 3A). The commercial rhUGT2B15 enzyme was not active against its probe substates (oxazepam, data not shown); thus, the role of UGT2B15 could not be measured using the recombinant system.

Enzyme Kinetics Parameters for DMA in rhUGT2B17, HIM, and HLM. DMA-G formation kinetic analysis in rhUGT2B17 showed V_{max} of 8 nmol/min per mg protein and the K_m of 1.63 μM (Fig. 3B). The kinetic parameters, i.e., V_{max} and K_m values for DMA-G formation in the high and null UGT2B17-expressing HIM, were 19.14 and 0.07 nmol/min per mg protein and 3.4 and 12.7 μM, respectively (Fig. 3C). Similarly, the V_{max} and K_m values in the high and null UGT2B17-expressing HLM were 27.4 and 3.8 nmol/min per mg protein and 4.4 and 5.9 μM, respectively (Fig. 3, D and G). Overall, intrinsic clearance in high compared with the null UGT2B17-expressing HIM and HLM was 1120- and 10-fold, respectively. Although UGT quantification was not the major goal of this work, we supplemented the enzyme kinetics data with proteomics information to demonstrate that only UGT2B17 protein abundance was different across null and high UGT2B17–expressing HIM and HLM, whereas UGT1A9, UGT2B17, and UGT2B15 abundance was comparable (Supplemental Table 7). The high and null UGT2B17-expressing HIMs and HLMs showed noticeable differences in K_m values, which is likely due to involvement of UGT1A9 in the null expressors.

Fraction of DMA Metabolized by UGT2B17 Enzyme in Intestine and Liver. The estimated $f_{m,\ UGT2B17}$ in intestine and liver microsomes was 99.6 and 86%, respectively, in the highest expressors (Fig. 4, E and F), thus suggesting a higher impact of UGT2B17-mediated metabolism in intestine compared with liver on DMA bioavailability.

Pharmacokinetic Analysis of DMA and DMA-G. The AUC of DMA-G (61.6 μmol × h/l) was 135-fold compared with DMA (0.45 μmol × h/l), further confirming glucuronidation as the major metabolic pathway of DMA (Fig. 4; Table 2). Similarly, the C_{max} of DMA-G (10.9 μmol/l) was 135-fold as compared with DMA (0.08 μmol/l). The elimination rate constant and half-lives were 0.21 $hours^{-1}$ and 3.5 hours and 0.1 $hours^{-1}$ and 4.7 hours for DMA and DMA-G, respectively.

Discussion

DMAU is a promising oral male hormonal contraceptive currently under clinical investigation. This study is the first to report the in vitro and in vivo metabolic characterization of DMA, which is the pharmacologically active metabolite of DMAU. The LC-HRMS analysis of human hepatocytes and serum samples revealed that glucuronidation is the major mechanism of DMA biotransformation. The in vitro screening results confirmed that UGT2B17 plays a primary role in metabolizing DMA to DMA-G. UGT2B17 is a highly variable enzyme with more than 3000-fold variability in its hepatic protein abundance (Oda et al., 2015), with a gene deletion frequency that varies with race by ∼16% in

TABLE 2

PK endpoints from the analysis of DMA and DMA-G samples following the oral administration of 100 mg DMAU

PK Endpoints (Mean ± S.D.)	DMA	DMA-G
$AUC_{0\text{-}24}$ (μmol/l per h)	0.45 ± 0.43	61.6 ± 18.6
C_{max} (μmol/l)	0.08 ± 0.08	10.9 ± 1.9
Elimination rate constant (h^{-1})	0.21 ± 0.07	0.1 ± 0.02
T_{max} (h)	6 ± 2	4.7 ± 3.1
T_{half} (h)	3.5 ± 0.98	7 ± 1.3

$AUC_{0\text{-}24}$, area under the systemic concentration-time profile curve of DMA (0-24 h); T_{half}, time taken for half the DMA concentration to be eliminated.

Caucasians to 96% in Asians (Xue et al., 2008). Therefore, we assessed the metabolism rates of DMA in the high versus null UGT2B17-expressing HIMs and HLMs, which showed >250- and sevenfold metabolism rates, respectively, in the high compared with null UGT2B17-expressors. This suggests that genetic polymorphism in UGT2B17 is likely leading to the variable DMA PK. Further, enzyme kinetics data were supplemented with proteomics information to demonstrate that only UGT2B17 protein abundance was different across null and high-UGT2B17 expressing HIM and HLM. The estimated $f_{m,\ UGT2B17}$ for intestinal and liver microsomes of the available highest expressors was 99.6 and 86%, respectively. Because UGT2B17 is mainly expressed in the intestine, it is likely that the intestine plays a major role in the first-pass elimination of DMA. Finally, human serum PK analysis showed that DMA-G AUC was >100-fold than DMA concentrations, which correlates with the extensive first-pass metabolism.

DMA is structurally similar to testosterone and retains the 17β-hydroxy group involved in glucuronidation. Accordingly, our hypothesis was that DMA is a substrate of UGT2B17, which leads to its high first-pass elimination and thereby poor and variable drug disposition. In addition to UGT2B17, we also found a minor contribution of UGT1A9 in the UGT screening assay of DMA; however, UGT1A9 is poorly expressed in intestine (Basit et al., 2020; Al-Majdoub et al., 2021), which makes it less relevant to the first-pass metabolism. Further, DMA kinetics data in HLM showed sevenfold higher metabolism rates in the high compared with null UGT2B17 expressors, which confirmed that UGT2B17 is the major enzyme involved in DMA metabolism, and UGT1A9 is a minor player despite its higher hepatic abundance. Although testosterone is also metabolized by UGT2B15 (Zhang et al., 2018), the HLM data from the high versus null UGT2B17-expressing donors suggest a negligible role of UGT2B15 in DMA metabolism. Interestingly, DMA is not metabolized by other androgen-metabolizing enzymes, unlike testosterone. In particular, testosterone is also metabolized by enzymes such as steroid 5α-reductase 2, cytochrome P450 3A4, sulfotransferase 2A1, and hydroxysteroid 17-β dehydrogenase 2 (Schiffer et al., 2018; Zhang et al., 2018). The potential reason for this discrepancy is the absence of the C-19 methyl group in DMA (Simard et al., 2005; Attardi et al., 2008; Han et al., 2021).

Considering that DMA is primarily metabolized by UGT2B17, it can be developed as a probe substrate for in vitro as well as in vivo studies to evaluate the effect of drug-drug interactions (DDIs) and genetic polymorphisms involving UGT2B17. Further, in the high UGT2B17 expressors, the magnitude of DDI needs critical evaluation because UGT2B17 inhibition can lead to dramatic increase in the systemic exposure of substrate in these individuals. Since DMA has been shown to be relatively safe in males, it can be used as a probe at lower doses for predicting DDI potential or UGT2B17 variability in males after further validation.

The role of UGT2B17 in variable drug PK has been shown to impact drug development. For example, an investigational asthma drug, MK-7246, showed 25-fold higher systemic exposure in subjects with UGT2B17 gene deletion compared with those with two gene copies (Wang et al., 2012). Additionally, UGT2B17 is involved in the metabolism of anticancer agents, such as vorinostat (Wong et al., 2011) and 17-hydroxyexemestane (Chen et al., 2016). Vorinostat PK is shown to be affected by UGT2B17 CNV, with UGT2B17*2 homozygotes exhibiting serious adverse events due to reduced glucuronidation rates and increased efficacy and toxicity as compared with subjects with one wild-type allele (Wong et al., 2011). The active metabolite of exemestane, 17-hydroxyexemestane showed significantly higher (>sixfold) exposure in patients homozygous for UGT2B17 deletion compared with those with two copies, likely due to reduced glucuronidation (Chen et al., 2016).

Further, UGT2B17 gene deletion is a key confounder in urinary antidoping testing, leading to potential false-negative and -positive results (Schulze et al., 2008; Kuuranne et al., 2014). The World Anti-Doping Agency screens for exogenous testosterone administration using the urinary ratio of deconjugated testosterone to epitestosterone (T/E ratio). This threshold for claiming testosterone supplementation was previously set to six in 1983 and was later reduced to four in 2005 (Mareck et al., 2010). However, baseline T/E ratio can differ by over 10-fold among different races (Jakobsson et al., 2006) and up to 20-fold between UGT2B17 deletion and high expressors (Schulze et al., 2008; Martín-Escudero et al., 2015). This also demonstrates the need for employing UGT2B17 biomarker to enable accuracy of doping tests by reducing the frequency of false-negative results in the deletion subjects with low or undistinguishable changes in T/E ratio.

Since DMA is a selective UGT2B17 substrate, it will likely exhibit high interindividual variability after oral dosing of DMAU, which can be considered for safe and cost-effective clinical trials (Fig. 5). First, subjects or patients can be stratified into null, mid, and high expressors of UGT2B17 for less variable and potentially safer clinical trials. Although such an approach adds the need for genotyping (Pereira et al., 2015), it is successfully implemented for other enzymes such as β2-adrenergic receptor (ADRB2) (Wechsler et al., 2009).

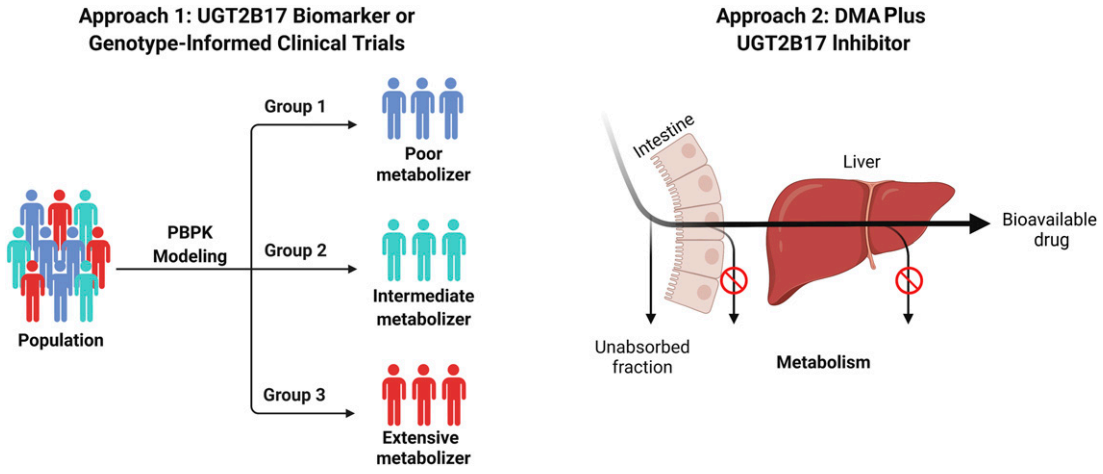

Fig. 5. Potential approaches to develop safe and effective oral DMAU delivery. In the first approach, subjects can be stratified into null, mid, and high expressors of UGT2B17 for effective clinical trials. Second, DMA can be administered with a specific UGT2B17 inhibitor to avoid the confounding effect of UGT2B17 metabolism in the first-pass elimination tissues such as intestine and liver.

Alternately, a selective UGT2B17 inhibitor can be used to avoid the variability from UGT2B17-mediated metabolism.

Physiologically based PK modeling, which accounts for the differences in the protein abundance of UGT2B17, and gene frequency, as well as other drug- and physiology-specific information, can be used to prospectively predict the effect of UGT2B17 genetic polymorphism and CNV on the drug PK when designing clinical trials. UGT2B17-mediated DDI potential can also be predicted using such an approach. The effect of enzyme inhibition by coadministered drugs as well as food, supplements, and intestinal diseases can also affect DMA metabolism due to their likely influence on intestine UGT2B17.

One of the limitations of this study was that the subjects were not genotyped for UGT2B17 due to the retrospective nature of the analysis. Although we could observe interindividual differences in the systemic profiles of DMA and DMA-G, future studies are warranted to systematically assess the effect of UGT2B17 genetic polymorphism. Moreover, we could only detect DMA-G metabolite in the human serum sample following DMAU oral administration, unlike testosterone. We could not detect androstenedione analog of DMA in the serum samples as opposed to the hepatocyte incubations, which is likely because the androstenedione analog is getting rapidly eliminated in sequential metabolic reactions. Nonetheless, the lack of C-19 methyl group in DMA structure provides a strong biochemical basis of the noninvolvement of other enzymes that metabolize testosterone.

In summary, we characterized the in vitro and in vivo metabolism of DMA, which revealed DMA-G as the major metabolite and a predominant role of intestinal and hepatic UGT2B17 in the metabolism. The elucidation of the DMA elimination pathways is crucial for individualized dosing and developing safer clinical trials. These findings are useful in building a top-down physiologically based PK model to understand the effect of UGT2B17 genetic polymorphism and CNV on DMA metabolism. The findings of this study can be applied for developing precision dosing and personalized medicine to achieve safe and predictable oral PK of DMAU during clinical trials.

Authorship Contributions

Participated in research design: Sharma, Wang, Lee, Blithe, Amory, Prasad.

Conducted experiments: Sharma, Ahire, Basit, Lajoie.

Performed data analysis: Sharma, Singh, Prasad.

Wrote or contributed to the writing of the manuscript: Sharma, Ahire, Basit, Lajoie, Wang, Lee, Blithe, Amory, Heyward, Prasad.

References

Ahire DS, Basit A, Karasu M, and Prasad B (2021) Ultrasensitive Quantification of Drug-metabolizing Enzymes and Transporters in Small Sample Volume by Microflow LC-MS/MS. *J Pharm Sci* **110**:2833–2840.

Al-Majdoub ZM, Scotcher D, Achour B, Barber J, Galetin A, and Rostami-Hodjegan A (2021) Quantitative Proteomic Map of Enzymes and Transporters in the Human Kidney: Stepping Closer to Mechanistic Kidney Models to Define Local Kinetics. *Clin Pharmacol Ther* **110**:1389–1400.

Amory JK (2020) Development of Novel Male Contraceptives. *Clin Transl Sci* **13**:228–237.

Attardi BJ, Engbring JA, Gropp D, and Hild SA (2011) Development of dimethandrolone 17beta-undecanoate (DMAU) as an oral male hormonal contraceptive: induction of infertility and recovery of fertility in adult male rabbits. *J Androl* **32**:530–540.

Attardi BJ, Pham TC, Radler LC, Burgenson J, Hild SA, and Reel JR (2008) Dimethandrolone (7alpha,11beta-dimethyl-19-nortestosterone) and 11beta-methyl-19-nortestosterone are not converted to aromatic A-ring products in the presence of recombinant human aromatase. *J Steroid Biochem Mol Biol* **110**:214–222.

Ayoub R, Page ST, Swerdloff RS, Liu PY, Amory JK, Leung A, Hull L, Blithe D, Christy A, Chao JH, et al. (2017) Comparison of the single dose pharmacokinetics, pharmacodynamics, and safety of two novel oral formulations of dimethandrolone undecanoate (DMAU): a potential oral, male contraceptive. *Andrology* **5**:278–285.

Basit A, Amory JK, and Prasad B (2018) Effect of Dose and 5α-Reductase Inhibition on the Circulating Testosterone Metabolite Profile of Men Administered Oral Testosterone. *Clin Transl Sci* **11**:513–522.

Basit A, Neradugomma NK, Wolford C, Fan PW, Murray B, Takahashi RH, Khojasteh SC, Smith BJ, Heyward S, Totah RA, et al. (2020) Characterization of Differential Tissue Abundance of Major Non-CYP Enzymes in Human. *Mol Pharm* **17**:4114–4124.

Blithe DL (2016) Pipeline for contraceptive development. *Fertil Steril* **106**:1295–1302.

Chen SM, Atchley DH, Murphy MA, Gurley BJ, and Kamdem LK (2016) Impact of UGT2B17 Gene Deletion on the Pharmacokinetics of 17-Hydroexemestane in Healthy Volunteers. *J Clin Pharmacol* **56**:875–884.

Daniels K, Daugherty J, Jones J, and Mosher W (2015) Current Contraceptive Use and Variation by Selected Characteristics Among Women Aged 15-44: United States, 2011-2013. *Natl Health Stat Rep* 1–14.

Han Y, Zhuang Q, Sun B, Lv W, Wang S, Xiao Q, Pang B, Zhou Y, Wang F, Chi P, et al. (2021) Crystal structure of steroid reductase SRD5A reveals conserved steroid reduction mechanism. *Nat Commun* **12**:449.

Jakobsson J, Ekström L, Inotsume N, Garle M, Lorentzon M, Ohlsson C, Roh H-K, Carlström K, and Rane A (2006) Large differences in testosterone excretion in Korean and Swedish men are strongly associated with a UDP-glucuronosyl transferase 2B17 polymorphism. *J Clin Endocrinol Metab* **91**:687–693.

Kuuranne T, Saugy M, and Baume N (2014) Confounding factors and genetic polymorphism in the evaluation of individual steroid profiling. *Br J Sports Med* **48**:848–855.

Ladumor MK, Bhatt DK, Gaedigk A, Sharma S, Thakur A, Pearce RE, Leeder JS, Bolger MB, Singh S, and Prasad B (2019) Ontogeny of Hepatic Sulfotransferases and Prediction of Age-Dependent Fractional Contribution of Sulfation in Acetaminophen Metabolism. *Drug Metab Dispos* **47**:818–831.

Mareck U, Geyer H, Fusshöller G, Schwenke A, Haenelt N, Piper T, Thevis M, and Schänzer W (2010) Reporting and managing elevated testosterone/epitestosterone ratios–novel aspects after five years' experience. *Drug Test Anal* **2**:637–642.

Martín-Escudero P, Muñoz-Guerra J, Del Prado N, Galindo Canales M, Fuentes Ferrer M, Vargas S, Soldevilla AB, Serrano-Garde E, Miguel-Tobal F, Maestro de Las Casas M, et al. (2015) Impact of UGT2B17 gene deletion on the steroid profile of an athlete. *Physiol Rep* **3**:e12645.

Oda S, Fukami T, Yokoi T, and Nakajima M (2015) A comprehensive review of UDP-glucuronosyltransferase and esterases for drug development. *Drug Metab Pharmacokinet* **30**:30–51.

Pereira NL, Sargent DJ, Farkouh ME, and Rihal CS (2015) Genotype-based clinical trials in cardiovascular disease. *Nat Rev Cardiol* **12**:475–487.

Prasad B, Achour B, Artursson P, Hop CECA, Lai Y, Smith PC, Barber J, Wisniewski JR, Spellman D, Uchida Y, et al. (2019) Toward a Consensus on Applying Quantitative Liquid Chromatography-Tandem Mass Spectrometry Proteomics in Translational Pharmacology Research: A White Paper. *Clin Pharmacol Ther* **106**:525–543.

Schiffer L, Arlt W, and Storbeck K-H (2018) Intracrine androgen biosynthesis, metabolism and action revisited. *Mol Cell Endocrinol* **465**:4–26.

Schulze JJ, Lundmark J, Garle M, Skilving I, Ekström L, and Rane A (2008) Doping test results dependent on genotype of uridine diphospho-glucuronosyl transferase 2B17, the major enzyme for testosterone glucuronidation. *J Clin Endocrinol Metab* **93**:2500–2506.

Simard J, Ricketts M-L, Gingras S, Soucy P, Feltus FA, and Melner MH (2005) Molecular biology of the 3beta-hydroxysteroid dehydrogenase/delta5-delta4 isomerase gene family. *Endocr Rev* **26**:525–582.

Surampudi P, Page ST, Swerdloff RS, Nya-Ngatchou JJ, Liu PY, Amory JK, Leung A, Hull L, Blithe DL, Woo J, et al. (2014) Single, escalating dose pharmacokinetics, safety and food effects of a new oral androgen dimethandrolone undecanoate in man: a prototype oral male hormonal contraceptive. *Andrology* **2**:579–587.

Thirumalai A, Ceponis J, Amory JK, Swerdloff R, Surampudi V, Liu PY, Bremner WJ, Harvey E, Blithe DL, Lee MS, et al. (2019) Effects of 28 Days of Oral Dimethandrolone Undecanoate in Healthy Men: A Prototype Male Pill. *J Clin Endocrinol Metab* **104**:423–432.

Wang Y-H, Trucksis M, McElwee JJ, Wong PH, Maciolek C, Thompson CD, Prueksaritanont T, Garrett GC, Declercq R, Vets E, et al. (2012) UGT2B17 genetic polymorphisms dramatically affect the pharmacokinetics of MK-7246 in healthy subjects in a first-in-human study. *Clin Pharmacol Ther* **92**:96–102.

Wechsler ME, Kunselman SJ, Chinchilli VM, Bleecker E, Boushey HA, Calhoun WJ, Ameredes BT, Castro M, Craig TJ, Denlinger L, et al.; National Heart, Lung and Blood Institute's Asthma Clinical Research Network (2009) Effect of beta2-adrenergic receptor polymorphism on response to longacting beta2 agonist in asthma (LARGE trial): a genotype-stratified, randomised, placebo-controlled, crossover trial. *Lancet* **374**:1754–1764.

Westaby D, Ogle SJ, Paradinas FJ, Randell JB, and Murray-Lyon IM (1977) Liver damage from long-term methyltestosterone. *Lancet* **2**:262–263.

Wong N-S, Seah EZh, Wang L-Z, Yeo W-L, Yap H-L, Chuah B, Lim Y-W, Ang PC, Tai B-C, Lim R, et al. (2011) Impact of UDP-gluconoryltransferase 2B17 genotype on vorinostat metabolism and clinical outcomes in Asian women with breast cancer. *Pharmacogenet Genomics* **21**:760–768.

Xue Y, Sun D, Daly A, Yang F, Zhou X, Zhao M, Huang N, Zerjal T, Lee C, Carter NP, et al. (2008) Adaptive evolution of UGT2B17 copy-number variation. *Am J Hum Genet* **83**:337–346.

Zhang H, Basit A, Busch D, Yabut K, Bhatt DK, Drozdzik M, Ostrowski M, Li A, Collins C, Oswald S, et al. (2018) Quantitative characterization of UDP-glucuronosyltransferase 2B17 in human liver and intestine and its role in testosterone first-pass metabolism. *Biochem Pharmacol* **156**:32–42.

Address correspondence to: Dr. Bhagwat Prasad, Department of Pharmaceutical Sciences, Washington State University, 412 E Spokane Falls Blvd, Spokane, WA 99202. E-mail: bhagwat.prasad@wsu.edu